aBio: Active Bi-Olfactory Display using Subwoofers for Virtual Reality

You-Yang Hu[1] Yao-Fu Jan[1] Kuan-Wei Tseng[1] You-Shin Tsai[1]
Hung-Ming Sung[1] Jin-Yao Lin[2] Yi-Ping Hung[1]

[1]National Taiwan University, Taipei, Taiwan [2]Tainan National University of Arts, Tainan, Taiwan

hung@csie.ntu.edu.tw

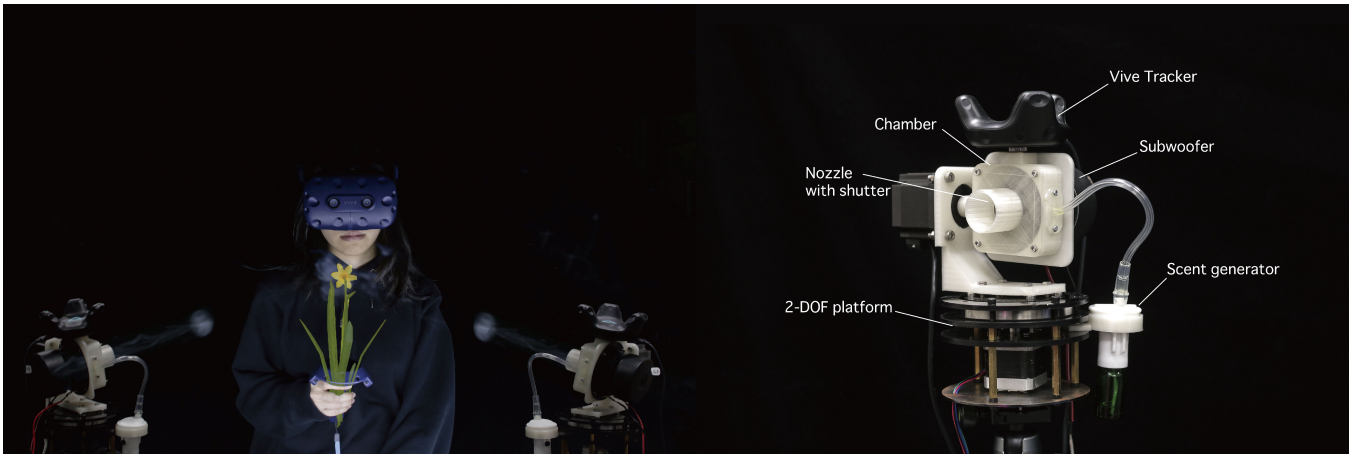

Figure 1: Proposed active bi-olfactory display system (aBio). The left side shows the scenario of presenting a virtual flower's smell in front of a user's nose. The right side is the configuration of the proposed olfactory display unit.

ABSTRACT

Including olfactory cues in virtual reality (VR) would enhance user immersion in the virtual environment, and precise control of smell would facilitate a more realistic experience for users. In this paper, we present aBio, an active bi-olfactory display system that delivers scents precisely to specific locations rather than diffusing scented air into the atmosphere. aBio provides users with a natural olfactory experience in free air by colliding two vortex rings launched from dual speaker-based vortex generators, which also has the effect of cushioning the force of air impact. According to the various requests of different applications, the collision point of the vortex rings can be positioned anywhere in front of the user's nose. To verify the effectiveness of our device and understand user sensations when using different parameters in our system, we conduct a series of experiments and user studies. The results show that the proposed system is effective in the sense that users perceive smell without sensible haptic disturbance while the system consumes only a very small amount of fragrant essential oil. We believe that aBio has great potential for increasing the level of presence in VR by delivering smells with high efficiency.

CCS CONCEPTS

• **Hardware → Analysis and design of emerging devices and systems**; • **Human-centered computing → Interaction devices**.

KEYWORDS

olfactory experience, olfactory display, vortex generator, vortex ring, virtual reality

ACM Reference Format:
You-Yang Hu, Yao-Fu Jan, Kuan-Wei Tseng, You-Shin Tsai, Hung-Ming Sung, Jin-Yao Lin, and Yi-Ping Hung . 2021. aBio: Active Bi-Olfactory Display using Subwoofers for Virtual Reality. In *Proceedings of the 29th ACM International Conference on Multimedia (MM '21), October 20–24, 2021, Virtual Event, China.* ACM, New York, NY, USA, 9 pages. https://doi.org/10.1145/3474085.3475678

1 INTRODUCTION

Compared with the highly active development of VR techniques for visual, auditory, and even haptic sensations, the development of olfactory displays is slow but steady. Augmenting auditory and haptic cues with olfactory cues would deepen viewers' understanding and sense of reality [5, 9]. This is achievable via the use of an olfactory display, a device which generates scents and stimulates humans' olfactory organs.

MM '21, October 20–24, 2021, Virtual Event, China

ACM ISBN 978-1-4503-8651-7/21/10…$15.00
https://doi.org/10.1145/3474085.3475678

Many existing olfactory displays use wind to diffuse scents into the air using fans [7, 38]; these are known as environmental-type displays, and are effective at presenting ambient odors. However, such diffusion of scent molecules spreads odors throughout the entire space and it is difficult to eliminate the odor from the air.To solve this problem, wearable olfactory displays have been developed which present the odor directly to the user's nose [16, 27, 41]. Thus injecting the smell into the user's nose makes it easier to control the olfactory information. Nonetheless, the user must bear the burden of an olfactory device in addition to the head-mounted display, which tends to deteriorate the natural sensory experience in VR.

In light of these difficulties, there has been a growing interest in the vortex-type display. A vortex is a fluid-mechanical phenomenon in which a region of fluid rotates around an axis line. Scent molecules are sealed in the vortex ring and delivered to the user via airflow. The odor is released once the vortex ring has collapsed by collision. To generate a vortex ring, scented air molecules must be exhausted from a semi-enclosed chamber at high speed. Many approaches utilize an air vortex cannon to produce vortex rings. These generally rely on a piston-driven slider crank to expel the odor from the chamber. Another solution is acoustically-driven vortex generator based on loudspeaker, in particular, subwoofer. Subwoofer convert electrical energy into mechanical vibration which compresses and projects air molecules from the chamber. In comparison to the piston mechanism, the subwoofer driven vortex generator has more potential application, such as the sound system that capable of olfactory display and we can modify the input wave signal to create different launch configurations.

In this paper, we present an olfactory display system (aBiO) that projects smells of virtual objects and provides users with an interactive olfactory experience in VR. As shown in Fig. 1, scented vortex rings launched from two subwoofer driven olfactory displays collide in mid-air to release smell. The airflow momentum is eliminated by the collision of two vortex rings, thus reducing unnatural and disturbing haptic sensation. The collision point is precisely positioned in front of the user to maximize olfactory sensation while minimizing haptic sensation. In contrast to other types of olfactory displays, the proposed system consumes a very small amount of liquid odorant to provide the user with mid-air scents.

Experimental analysis shows that the proposed system achieves precise localization of the smell in three-dimensional space. According to the design principle of the user-centered olfactory display, the smell can be released anywhere in front of the user's nose at any time. Additionally, we conduct pilot and user studies to evaluate the correlation between significant system parameters and human sense. This serves as a design guideline for implementations or extensions of the proposed olfactory display system.

2 RELATED WORKS

2.1 Olfactory Displays for Multimedia

In the human-computer interface field, an olfactory display is defined as a computer-controlled system with hardware, software, and chemicals that presents olfactory sensations to humans [5]. Compared with other types of displays (e.g., visual and auditory), although olfaction—that is, the sense of smell—is inherently complex as a media component, numerous olfactory displays have been developed for multimedia. Existing olfactory displays can be largely categorized into environmental displays, placed in the environment, and wearable displays, equipped on the body or on the head [25].

2.1.1 Environmental Olfactory Displays.

Stationary environment olfactory displays typically rely on airflow to carry the scents to the user's nose. Beginning with Sensorama [17], an immersive system that utilized an air conditioning system to deliver smell released from vials for a multi-sensory experience, several techniques have been developed that use wind to present smells [7, 10, 14, 30, 34, 38]. This approach's primary advantage is in its unobtrusive nature: the user may even be unaware of the the presence of the olfactory display. With this advantage, however, comes the the difficulty of precisely positioning an odor at a specific location. Although these approaches [15, 21, 23] facilitate the spatial control of smell, they require a large amount of liquid perfume to ensure continuing operation, which causes scents to linger in the air. To solve these problems, [18, 29, 37] have developed olfactory displays based on inkjet technology. However, due to the device's range and fixed limitations, the user must sit in front of it, which makes it difficult to provide an olfactory experience within a movable area.

2.1.2 Wearable Olfactory Displays.

Wearable olfactory displays also provide users with an olfactory experience. These can be further divided into on-body and head-mounted displays. For example, [6, 41] reported the backpack-mounted devices that dictated the strength and timing of odor presentation based on user's location in the virtual environment. More recently, several personal on-body olfactory devices [1, 2, 39] are developed for VR therapy, psychotherapy, and social interaction. Following the development of VR head-mounted display (HMD) technology, many head-mounted olfactory displays have been proposed. For example, [16] have proposed an HMD olfactory display that uses a surface acoustic wave (SAW) device based on previous research [3, 4]. This olfactory display provides the user with scents vaporized from a SAW device with low liquid perfume consumption. [22] reflects scent-emitting sources intensities based on environment fluid dynamic simulation. HMD olfactory displays [8, 20, 28, 32] have also been developed to explore the connection between human olfaction and other senses. Compared with stationary environmental olfactory displays, the wearable approach facilitates precise control of smell in terms of time, position, and intensity, as the scent is directly released to the user's nose. However, users must wear an additional olfactory device, which many users find uncomfortable and intrusive, thus hindering immersion in the virtual environment.

2.1.3 Vortex based Olfactory Display.

To address the limitations of these two types of olfactory displays, Watkins proposes a system that uses a vortex ring to present scents [40]. Based on this concept, [45] proposed the "Scent Projector", composed of a vision-based nose tracker, a steerable accordion air cannon, and a commercially available scent diffuser. This presents a smell in front of the user's nose through a scented vortex ring launched by the air cannon. However, intense air pressure results when the vortex ring encounters the user's face. Also, due to tracking limitations, it cannot be applied to moving users. To

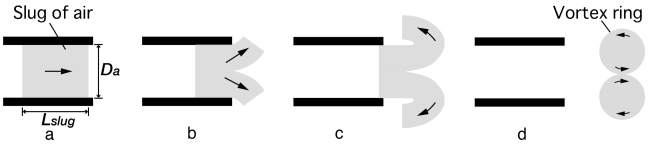

Figure 2: Fluid ejected from a nozzle forms into a vortex ring

reduce this haptic sensation, Nakaizumi et al. have two vortex rings collide [26]: when the vortexes collide, the strong vortex airflow decelerates into a scented breeze and releases an olfactory field in front of the user's face. [44] further use a pilot study to prove that the airflow direction after vortex collision can be controlled by adjusting the velocity of the vortex rings. To address the tracking limitation, [24] proposed an olfactory display to deliver scented vortex rings to a walking person. The system uses a time-of-flight camera to track the moving user's distance within a specific area. Vortex based olfactory displays include a novel way to achieve spatio-temporal control of olfactory stimuli, and does not require the user to wear any physical devices.

2.2 Acoustically Driven Vortex Generators

Outside of the context of olfactory displays, our work draws from applications based on the acoustically driven vortex cannon [13, 19, 31, 33]. This type of vortex generator simply uses the vibrations of a speaker diaphragm to squeeze the air out of a chamber to generate the vortex ring. Compared with piston-driven vortex generators used in most olfactory displays [24, 26, 43–45], speaker based vortex generators has more potential application. For example, [33] developed robots that used speaker-based vortex generator for communication. [19] used the collision of two vortex rings for visual content projection. [13, 36] developed haptic devices using the speaker-based vortex generator. In point of fact, each of the studies described above used acoustically driven vortex generators optimized for an specific application – communication, projection, and haptic feedback, respectively – except odor delivery, which motivating our design of a speaker based vortex generator specifically for olfactory display system.

3 PRELIMINARIES

3.1 Vortex Formulation

A vortex ring is an annular airflow, usually in the shape of toroid (or a "doughnut"). The vortex formation process is illustrated in in Fig. 2. A slug of air is rapidly ejected from a circular aperture (Fig. 2a). When the air slug leaves the aperture (Fig. 2b), its outer edge moves slower than the inner edge due to the aperture's friction, causing the outer edge to curl outwards (Fig. 2c) [35]. The air continues to rotate until it accumulates into a vortex ring which pinches off from the aperture (Fig. 2d). This rotation allows the vortex ring to travel in a stable shape for an extended distance. As the vortex is composed of the air at the aperture, the odor can be encapsulated in the vortex ring and then projected to the space beyond the aperture [42]. The scent inside is released only when the vortex ring is collapsed. As such, the vortex is an ideal medium for accurate odor delivery.

To make a vortex ring move to a target without deviating from its trajectory or self-dissipating halfway, we must design a vortex generator that can launch a stable vortex ring. In fluid dynamics, the classical model of a vortex generator is a tube with a piston inside and a circular aperture at the end (Fig. 2a). The stroke ratio, that is, the ratio between the length of the slug L_{slug} and the aperture diameter D_a, determines the stability of the vortex ring [11]:

$$R_{\text{stroke}} = \frac{L_{\text{slug}}}{D_a} \tag{1}$$

Assuming that the air pushed out of the aperture is incompressible, we can calculate the length of the slug by the total air volume V_{slug} leaving the aperture and the area S_a of the circular aperture [12, 35].

$$L_{\text{slug}} = \frac{V_{\text{slug}}}{S_a} = \frac{4V_{\text{slug}}}{\pi D_a^2} \tag{2}$$

From Eq.1 and Eq.2, we can express the stroke ratio as:

$$R_{\text{stroke}} = \frac{4V_{\text{slug}}}{\pi D_a^3} \tag{3}$$

which is the key to optimizing the design of the vortex generator. For a stable vortex ring, the stroke ratio must be smaller than a theoretically defined threshold (called the formation number) which is between 3.6 and 4.5 [11]. As previously mentioned, we have found no prior study that theoretically analyzes the relationship between the stroke ratio and the design of the olfactory vortex generator. Hence in the next section, we experimentally calibrate the stroke ratio parameters to optimize the design of the vortex generator.

4 PRECISION OLFACTORY DISPLAY

We developed a subwoofer-driven olfactory display that precisely delivers the air vortex of the scents, both in terms of location and time. Fig. 3 shows the workflow of the proposed olfactory display. A tiny scent droplet is produced by a controllable scent generator and then transmitted into an airtight chamber of the vortex generator. The smell is not released until the shutter is opened, at which time the subwoofer vibrates to compress the air, forming a vortex ring which carries the odor molecules to the target location.

Our olfactory display is composed of two main parts: a scent generator, and a vortex generator with a 2-DOF platform.

4.1 Scent Generator

In our olfactory display, the scent generator atomizes the odor solution into tiny odor droplets and transmits them to the vortex generator. It produces deliverable odor molecules from odor sources with low consumption and high efficiency and achieves precise control of the concentration during the generation process.

The scent generator configuration is shown in Fig. 3a. It is composed of a container, an air pump, and an atomizer. The system uses a pump motor to generate a stable compressed airflow. Based on Bernoulli's principle, the vacuum suction generated by the compressed air flow draws the scented liquid from the container to the atomizer inlet at the top, after which the liquid is atomized into very fine droplets by collision and then released to the outside through a tube. Many kinds of scented liquids can be used in this, including essential oils or alcohol-soluble fragrance liquids. Note that if pure essential oils are used in this system, there is no need to add water, heat, or use alcohol for dilution, which means the system maximizes the efficiency of essential oil-based scent production, and yields pure odors. With this approach, another advantage as that if

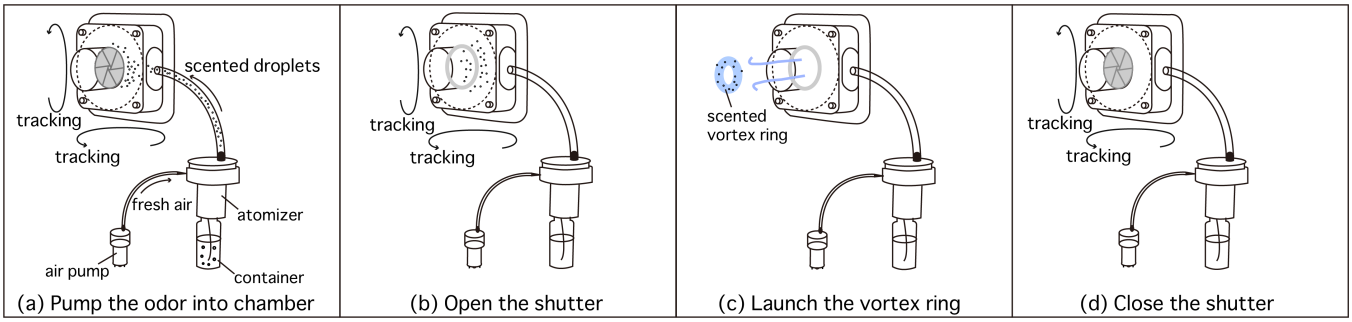

Figure 3: System Workflow

the compressed air flow generated by the pump motor remains unchanged, the production rate of the scented molecules is constant; thus, controlling the operation time of the pump motor allows for precise control of the concentration of the scented droplets.

4.2 Vortex Generator with Platform

In this part, the vortex generator launches the vortex ring, which contains the odor droplets generated by the scent generator. As shown in Fig. 1, this consists of a 0.1 L cylindrical chamber, a nozzle with a Canon™ shutter, a 3-inch 20 W Ouxiang™ speaker, a 2-DOF platform, and a Vive Tracker. All components except the shutter, the speaker, the platform, and the Vive Tracker were 3D printed on an Anycubic™ printer using 1.75 mm Esun™ polylactic acid material. The speaker was installed opposite to the aperture to function as a piston, flexing the diaphragm to push air out of the chamber to generate the vortex ring. To control the flight trajectory of the vortex ring, we mounted the vortex generator on a self-made electric 2-DOF platform equipped with two stepping motors, allowing for precise control of the rotation of the vortex generator. In addition, the shutter allowed us to control the opening and closing of the aperture to prevent scented air from leaking during filling.

Several cores of our vortex generator design are smaller in size, produce less noise, and can deliver more odor in a single launch. The most important feature is producing a stable vortex ring to achieve precise olfactory display. Equation 3 from the previous section shows that the stability of the launched vortex ring is related to the aperture size and the air volume leaving the aperture. Furthermore, the literature indicates that the stability of the launched vortex ring is also affected by the nozzle shape and the diaphragm velocity [45], and is not significantly affected by the inner volume of the enclosure [46]. Therefore, we first arbitrarily set the chamber volume to 0.1 L to reduce the total size of the generator. Next, we conducted three experiments to find the optimal design for our olfactory vortex generator.

4.2.1 *Air Volume Measurement.*

To maximize the volume of scent delivered during each launch, we first conducted an experiment to measure the maximum air slug volume pushed by the diaphragm. As the surface of the speaker diaphragm is not flat, it is not practical to calculate the pushed air slug volume by measuring the diaphragm displacement. Thus we built a device consisting of the same chamber used for the vortex generator and a needle tube with an inside diameter D_{tube} of 30 mm. Assuming that the air pushed out of the aperture is incompressible, we obtain the total pushed air slug volume by measuring the displacement of the needle piston H_{piston}. The speaker diaphragm's movement is triggered by a positive square pulse signal generated using Python. We control the diaphragm displacement by adjusting the duration of the square wave. Notably, we found that the duration of 40 ms produced the greatest needle piston displacement; increasing the amplitude beyond 40 ms can not increase the amount of the needle piston movement. We thus obtained 9 mm as the value of H_n. For our vortex generator, the maximum volume of air slug V_{slug} displaced by the speaker diaphragm can be computed as

$$V_{\text{slug}} = \pi \left(\frac{D_{\text{tube}}}{2} \right)^2 \times H_{\text{piston}} = \pi \times (15)^2 \times 9 = 110\text{mm}^3 \quad (4)$$

4.2.2 *Aperture Selection.*

We further conducted an experiment to determine the aperture diameter and shape that produce the most stable and high concentration scented vortex ring. For the aperture diameter, from Equation 3 and V_{slug}, we preliminarily calculated that the aperture diameters fall between 28 mm to 30 mm, which corresponds to the formation number ranging from 3.6 to 4.5, which as mentioned above are the theoretically defined threshold to obtain a stable vortex ring. As for the aperture shape, the literature indicates that a vortex generator with the aperture extruding from the body launches a more stable vortex ring, and that a curved shape produces more haptic sensations than a flat one [36]. In contrast to vortex-based haptic devices, olfactory displays should minimize haptic sensations caused by the vortex ring. Thus we decided on a flat shape nozzle with the aperture extruding from the body. Note that we found no studies detailing how the extruded length of the flat shape affects the stability of a vortex ring; nor did we find any studies evaluating the relationship between the scent intensity of the vortex ring and the aperture parameters. Hence we evaluated nine different apertures with diameters ranging from 28 mm to 30 mm and nozzle lengths ranging from 20 mm to 40 mm.

To evaluate the accuracy and relative scent concentration carried by the vortex rings launched using different apertures, we built the electronic nose shown in Fig. 4a. Since it is difficult to find a instrument that can sense arbitrary odor molecules, we use alcohol instead. It consists of nine high-sensitivity alcohol sensors (MQ3) aligned in a 3x3 matrix. The distance between each sensor unit is 35 mm. The effective measuring range of this sensor is 0.05 mg/L

	Square			Clipped Sine			Clipped Sinc			Clipped Sinc with Hamming Window		
Duration (ms)	Noise (dB)	Accuracy (%)	Occ (mg/L)	Noise (dB)	Accuracy (%)	Occ (mg/L)	Noise (dB)	Accuracy (%)	Occ (mg/L)	Noise (dB)	Accuracy (%)	Occ (mg/L)
50	75.1	100	1.72	64.8	100	1.6	63.3	100	1.63	61	100	1.63
60	74.8	100	1.69	63	100	1.62	62.5	100	1.51	59.6	100	1.54
70	75.2	95	1.76	61.5	90	1.49	61.3	90	1.41	59.2	95	1.46

Table 1: Signal waveform selection experiment results. (Occ: Odor carrying capacity). The ambient noise level was 42 dB.

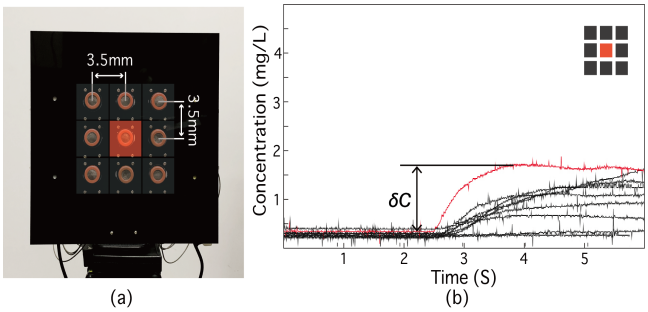

Figure 4: (a) Electronic nose (b) Successful hit case

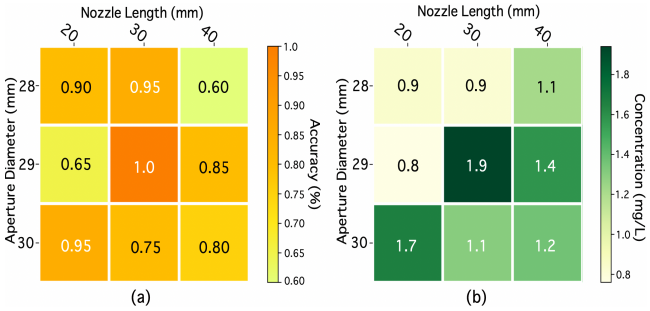

Figure 5: (a) Accuracy result (b) Concentration result

to 10 mg/L. The nine sensors' detect concentrations were sent to a data visualization program running on PC by an ESP32 module. As shown in Fig. 4b, the results of the center sensor were visualized in a red line. When the vortex ring collides with the electronic nose, the status of lines reflected the concentration distribution. Hence, by analyzing the line that increased the most, we obtain the exact collision area. For detailed illustration of the electronic nose's data visualization, please refer to the supplementary. As shown in Fig. 4b, a case was considered a successful hit only when the red line increased first and highest. And we can obtained the relative carried concentration by calculating the difference from a stable state to the peak(δC).

The experiment was conducted in a windless environment. The olfactory display was placed 70 cm away from the electronic nose. We turned on the scent generator's air pump for 3 s to fill the chamber with 99% alcohol droplets, after which we launched the vortex ring to the electronic nose. Note that in this experiment, we used a 60 ms duration square pulse signal to drive the subwoofer. Each type of aperture was repeated 20 times using this process. Given the detection data on the electronic nose, we calculated the successful hit rate and the average concentration under the successful hits. As shown in Fig. 5, the aperture with a 29 cm diameter and a 30 cm length provided the most efficient and accuracy scented vortex ring. Thus we used this aperture for further olfactory display design.

4.2.3 *Signal Waveform Selection.*

One of the limitations in acoustically driven vortex generator is the bump sound produced by the speaker diaphragm, which interrupts the user's sense of immersion in the VR experience. However, we found no previous studies that attempted to mute this loud noise. The electric impulse wave signal driving the movement of the speaker diaphragm is the key to minimizing this noise. In contrast to previous works [13, 33] that used square wave to flex the speaker diaphragm in and out, we tested a variety of different waveforms which have fewer high-frequency signals. Fourier analysis of the square wave reveals high-frequency components, which could cause audible noise. In contrast, the sine and sinc wave produces fewer audible sounds, and thus could yield quieter operation during the launch of the vortex generator. Another issue is that when using waves to generate the vortex, negative amplitudes hinder the creation of the vortex ring. Therefore, we adopted a Hamming window on the sinc wave, taking the positive central part as our pulse signal to drive the speaker movement.

To verify the noise reduction for this method and choose the best pulse signal, we used the decibel meter (TM-101) and the electronic nose placed 70 cm away from the vortex generator to measure the sound intensities, accuracy, and odor carrying capacity under four waveforms of pulse signals (square, sine, sinc, sinc with Hamming window) in different durations. Notably, to keep the diaphragm at the maximum displacement long enough to launching a stable vortex ring, we amplified all waveform signals by 6 dB to become clipped signals. All signals were generated using Python and exported as wav files for the subwoofer to play. Table 1 shows the results produced with four waveforms in three different durations(50 ms, 60 ms, 70 ms), for more results in longer duration, please refer to the supplementary. The measurement results show that clipped sine, clipped sinc, and clipped sinc with Hamming window pulse signals were all effective in reducing noise, and their accuracy can reach 100% in the duration of 60 ms and below. In most cases, a shorter duration meant that the vortex ring could carry more odor, but it would produce a louder sound. Since accuracy and minimal noise were our primary concerns, we decided to use the 60 ms clipped sinc with Hamming window wave, which reduced

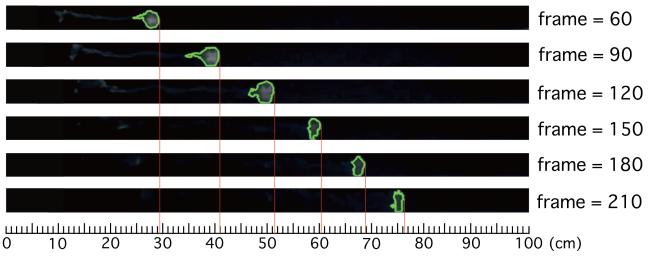

Figure 6: Vortex ring position at different time points.

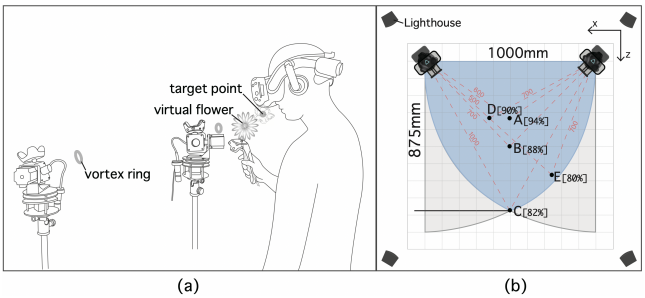

Figure 7: (a)System concept (b)System top view

the maximum launch noise by 15 dB compared with the square wave, and it had 100% accuracy.

4.2.4 *Vortex Ring Movement.*

In the system with two olfactory display units, we want to make the vortex rings collide at the target point: to do this we must ensure that the vortex rings reach the target collision point at the same time. Since the distance between the collision point and each generator is not always the same, we must determine the relationship between the reach distance and the elapsed time of the launched vortex rings. Given this relation, we can control the launch time of each vortex ring to cause them to both reach the collision point at the same time. To measure this relationship, we first revealed the vortex ring using stage smoke (S-400W) and then captured the movement of the vortex ring with a camera (iPhone X rear lens) at 240 fps. We analyzed this video using image processing, thresholding the greyscaled video clip to determine the position of the largest contour of the vortex ring in each frame, as illustrated in Fig. 6. We converted the image pixels to actual distances to yield the real distance and time relationship. Finally, we used regression to calculate the following time-distance formula of the vortex:

$$y = 3.629e-07x^3 + 1.509e-05x^2 + 0.008438x - 0.01392, \quad (5)$$

based on which, given a certain distance, we can accurately control the launch time of the two vortex generators.

4.3 Bi-Olfactory Display System

4.3.1 *System Concept.*

aBio can generate the smell at a specific target point via a mid-air collision of two vortex rings. Fig. 7b shows the concept of this system. It consists of two olfactory display units. Each olfactory display unit launches the vortex ring at the target point. The local high-speed airflow that forms the vortex ring is interrupted when two vortex rings collide with each other, creating an . The 2-DOF platform controls the rotation of the vortex generator, which allows the vortex ring to be directed to a specific target point in a certain range of 3D space. Through precise vortex control and Vive's tracking technology, aBio can synchronize the presentation of scents with the interactive plot of the moving user in VR, such as when the user picks up a virtual flower, the fragrance of flowers is presented around the user's nose.

4.3.2 *System Implementation.*

As shown in Figure 8, the system involves four main components: (1) The sound card (AUD) drives the two subwoofer speakers through a 3.5 mm stereo audio cable. (2) The ESP32 (buzzer firmware) controls air pumps that spread the odor into the chamber and switches the nozzle shutter. (3) The Arduino Uno (motor firmware) controls the vortex generator's horizontal and vertical rotation. These devices communicate with the VR system on the PC through a simple custom protocol via Wi-Fi and a USB serial port, respectively. (4) The interface script handles serial communication with embedded devices. VR Logic uses the interface script to send the rotation, launching, and charging commands to the firmware.

We combined the system with Vive tracking technology to enable the vortex generator to track the specific target collision point. We can use the tracker mounted on the vortex generator to track its rotation in real time. Moreover, we can define the collision point in the VR coordinate system and calculate the vector given the tracker and collision point's relative positions. In addition, we can use the head-mounted display position to track the user's nose in real-time and use this as the target collision point. We can also use the user-side controller's position to obtain the user's hand coordinate data to facilitate more interactive modes. For example, a user can smell the virtual object while holding it close to their nose. This approach helps aBio to significantly improve its spatial control of the smell and enables the user to experience interactive olfactory sensations without wearing additional olfactory devices.

5 SYSTEM EVALUATION

5.1 Collision Experiment

We first conducted an experiment to evaluate the collision accuracy of our system.

5.1.1 *Experiment Configuration.*

As shown in Fig. 7b, our experiments were conducted in a 1-m by 1-m space. The olfactory display unit's rotation range is ±45° on Y-axis, and ±40° on Z-axis. The maximum delivery distance is 875 mm, which is the forward distance from vortex generators, and the vertical direction is about ±770 mm. We chose five locations in the reachable area as collision points. Points A, B, and C are at the centerline between the two generators: their distances from the generators are 600 mm, 700 mm, and 1000 mm. Points D and E are at locations with different distances to each vortex generator; for these we set the launch time depending on the relation between the elapsed time and the reach distance determined in Section 4.2.4.

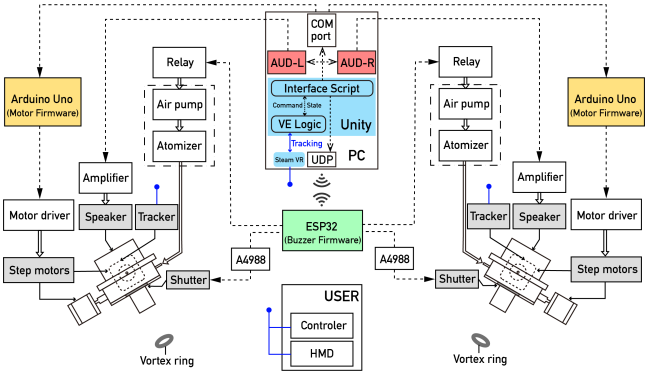

Figure 8: Overview of the architecture of aBio System.

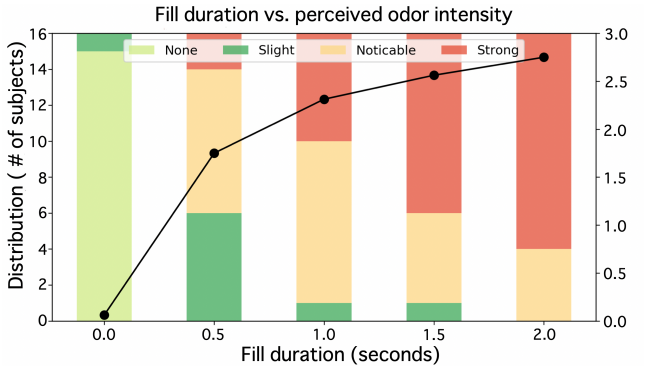

Figure 9: Pilot study results

5.1.2 Experiment Procedure.

We again used stage smoke to make the vortex visible and then launched the rings at target points. We repeated the experiment 50 times at each point to calculate the successful collision rate. There are three cases, the first case is that the two vortex rings successfully collapsed after collide, the second case is that the vortex rings miss completely, and the third case is that the vortex rings successfully collide but not collapsed. We only consider the first case as a successful collision. To make the experiment more objective, we recorded video of the collision process to check whether the vortex rings had collapsed after collide. For detailed illustration of the collision cases, please refer to the supplementary.

5.1.3 Results.

The results are also illustrated in Fig. 7b. In general, The average hit rate indicates that most of the vortex rings collided successfully since all of the hit rates were higher than 80%. From the results we observe two trends. First, the collision points with the same distance to each vortex generator (points A, B, and C) have higher average hit rates than the other collision points (points D, E). Second, collision points at farther distances had lower collision rates, since the flight stability of the vortex ring decreases with increasing distance.

5.2 Pilot Study

In our system, there are two ways to deliver the scent: (1) Set the vortex collision point on the virtual object to generate its olfactory field. (2) Set the vortex collision point in front of the user's nose to deliver the scent to the user. In this research, our goal is to develop an efficient olfactory display that the users can reliably smell the odor that the VR director would like them to perceive in a virtual environment. Therefore, we adopted the second approach which deliver the scent vortex directly in front of the user's nose.

We conduct some experiments to find the optimal parameters of the odor-filling duration and the vortex rings' collision distance from the user's nose. There are many controllable parameters that influence the actual and perceived odor intensity. Fill duration is one the most primary factors. Longer fill duration of odor can generally increase the odor intensity. Yet, it sacrifices the temporal continuity, i.e. the number of launches in a unit time, which may degrade the user experience. To this end, we first conduct a pilot study to find the optimal fill duration that can provide users a better olfactory experience. Also, we want to verify whether users can distinguish different intensity of the olfactory field through this experiment.

5.2.1 Experiment Configuration.

Our experiments were conducted in a 1-m by 1-m space. To ensure that no external airflow influenced the movement of the vortex rings' or the distribution of smell, the air conditioners were all turned off. Furthermore, to prevent participants from hearing the environmental noise, we supplied them with noise-cancelling headphones. We recruited 16 participants (7 males, 9 females) of a mean age 23 years old (SD=4.18). All participants are non-smokers with a normal sense of smell. Thirteen of these participants had experienced VR, four participants are VR developers. We set the fill duration to 0-2s, with 0.5s as the interval, and the collision point distance was 5cm from the area in front of the participants' nose. To enable participants to rate the perceived odor intensity, we defined four intensity levels: none (0), slight (1), noticeable (2), and strong (3) olfactory sensations, respectively.

5.2.2 Experiment Procedure.

At the experiment's beginning, we had the participants sit at point B, which was defined in collision experiment. And they were wearing the HMD with black scene displayed on it. In each round, we delivered to them 10 scented vortex rings (10 launches) with the same fill duration. For each launch, we guided the participants to inhale and exhale at certain timing to ensure that they were inhaling when the smell was released. There was a 20 seconds and 10 minutes rest between each launch and each round. Specifically for 10 minutes rest, they could smell the coffee beans or walk around to relieve their olfactory fatigue. The participants reported their average perceived intensity after each round. To regularize the result, there was a testing round with filling duration 2 seconds before the formal rounds start. We asked the participants to set the perceived intensity as strong (3). Afterwards, we conducted 5 rounds of experiments with 5 filling duration respectively.

5.2.3 Results.

The results are illustrated in Fig. 9. Theoretically, the delivered odor concentration is positively correlated to the run time of the pumping motor. The longer the motor runs, the more odor droplets are loaded into the chamber. We found that the average perceived odor intensity increases with the fill duration. However, the growth

becomes insignificant beyond a fill duration of 1.5 seconds since more than half of the participants experienced strong feelings. Although increasing fill duration contributes to better olfactory sensation, it may compromise the number of launches per unit time, which potentially reduces the temporal continuity of our device. However, in real life, when we pick up a flower to smell it, we do not always smell the flower's full fragrance; it can be a fleeting, intermittent experience. we will not always feel the fragrance of the flower. This kind of intermittent smell can increase the authenticity, As such an intermittent smell can be said to increase the authenticity of the experience, we chose a fill time of 2 seconds for the device to ensure a better olfactory experience for the user.

5.3 User Study

Based on the pilot study, we conducted a user study to determine the best collision distance. During the pilot study, many participants commented that it was difficult for them to assign scores representing the smell's intensity. Therefore, we changed the scoring question to a true/false question. To determine the best parameter, we asked participants at the end of the experiment which smell experience they felt to be most natural. We then used these participants' opinions to determine the best parameter value.

5.3.1 *Experiment Configuration.*

This experiment was conducted in the same setting as the pilot study. In order to ensure that the user's breathing rhythm would not affect the experiment, we had the participants worn head-phones with a voice guide played on it. We recruited 12 participants (5 males, 7 females) with a mean age of 22.75(SD=2.7). All participants were non-smokers with a normal sense of smell. Eight of these participants had experienced VR; of these two were VR developers. The test collision distance ranged from 5 cm to 17.5 cm—an increase of 2.5 cm. The odor fill time was fixed at 2 seconds.

5.3.2 *Experiment Procedure.*

We had the participants sit at same position as pilot study and wear the HMD with a virtual scene displayed on it. Each collision distance was tested 10 times, with 10 false launches as well to determine whether it was an outlier. In each test, a virtual flower floated towards the participants. If it was a true launch test, the devices launched when the flower approached. We disrupted the order of these 120 tests and asked after each launch if there was an odor, if the odor was too strong, and if there was an obvious haptic sensation. After each launch, the participants took a 20 seconds rest, and smelled the coffee beans to restore sense of smell. After completing the experiment, we asked them four questions: (1) How do you feel about smell in the experiment? (2) How you feel about the air columns hitting your face? (3) How long does the odor last? (4) What smell experience do you find most natural? For the detailed procedure flow of user study, please refer to the supplementary.

5.3.3 *Results.*

The results are shown in Fig. 10. We observe a logarithmic relationship between the probability of excessive odor and haptic detection rate as the collision distance decreases. However, as the collision distance *increases*, the probability of haptic detection and excessive odors increases linearly. The chart also shows that for collision distances greater than 17.5 cm, there is only a 50% chance

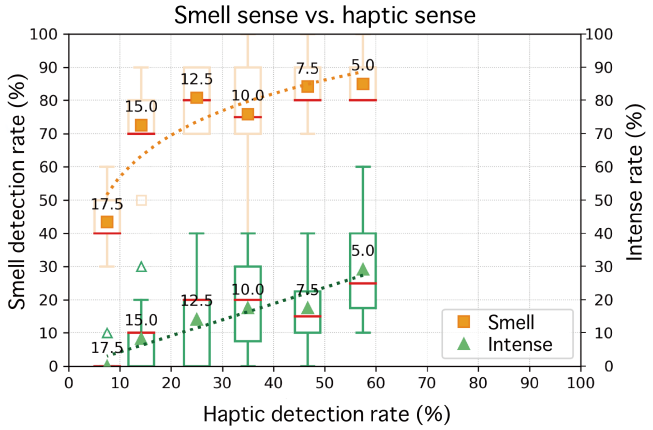

Figure 10: User study results

of smelling in each launch; for distances less than 12.5 cm, the probability increases to about 80%. Also, the probability of haptic detection and excessive odor increases as the distance decreases. However, in this chart we assume that every item of feedback is equally important. For a higher smell detection probability and reduced tactile sensation, the best parameter is closer to the upper-left corner, that is, a collision distance between 12.5 cm and 15 cm.

5.3.4 *Discussion.*

The above experimental results have helped us observe many correlations between our design configurations and human sensory perception. For the directors of VR works, this findings can be useful for those who want to use our system to deliver odors efficiently to the VR viewers. If the director does not care much about the user's haptic sensations and wants to increase the probability of the user's smelling the odor and to save the scent essence, he can set the vortex collision point at 12.5 cm. If the director wants to reduce the possibility of the user's sensing the vortex impact on the face when smelling the odor, he had better set the collision point at a farther away point, for example, at 15 cm.

6 CONCLUSION AND FUTURE WORKS

We propose aBio, an active bi-olfactory display system that demonstrates strong spatio-temporal control of scent delivery for virtual reality. Scent molecules are carried by vortex rings and released at designated collision points. Vortex collision significantly suppresses undesired airflow impact, reducing unwanted haptic feedback. We conduct pilot and user studies to determine the correlation between important design configurations and human sense. These parameters can be adjusted to satisfy the requirements of various applications. We believe that these results should be taken into account when designing virtual reality systems with olfactory experience.

In future works we would like to enabling the system to switch between odors in a short interval of time. We also want to extend aBio by adding more vortex cannons to create an ambi-olfactory display system with no blind spots. And with the advantage of the speaker's characteristics, we believe it is possible to design a sound system capable of the precisely olfactory display, which can provide users with a multi-sensory experience.

REFERENCES

[1] Judith Amores, Javier Hernandez, Artem Dementyev, Xiqing Wang, and Pattie Maes. 2018. Bioessence: A wearable olfactory display that monitors cardio-respiratory information to support mental wellbeing. In *2018 40th Annual International Conference of the IEEE Engineering in Medicine and Biology Society (EMBC)*. IEEE, 5131–5134.

[2] Judith Amores and Pattie Maes. 2017. Essence: Olfactory interfaces for unconscious influence of mood and cognitive performance. In *Proceedings of the 2017 CHI conference on human factors in computing systems*. 28–34.

[3] Yossiri Ariyakul and Takamichi Nakamoto. 2011. Olfactory display using a miniaturized pump and a SAW atomizer for presenting low-volatile scents. In *2011 IEEE Virtual Reality Conference*. IEEE, 193–194.

[4] Yossiri Ariyakul and Takamichi Nakamoto. 2013. Improvement of odor blender using electroosmotic pumps and SAW atomizer for low-volatile scents. *IEEE Sensors Journal* 13, 12 (2013), 4918–4923.

[5] Woodrow Barfield and Eric Danas. 1996. Comments on the use of olfactory displays for virtual environments. *Presence: Teleoperators & Virtual Environments* 5, 1 (1996), 109–121.

[6] John P Cater. 1994. Smell/taste: odors in reality. In *Proceedings of IEEE International Conference on Systems, Man and Cybernetics*, Vol. 2. IEEE, 1781–vol.

[7] Yang-Sheng Chen, Ping-Hsuan Han, Kong-Chang Lee, Chiao-En Hsieh, Jui-Chun Hsiao, Che-Ju Hsu, Kuan-Wen Chen, Chien-Hsing Chou, and Yi-Ping Hung. 2018. Lotus: enhancing the immersive experience in virtual environment with mist-based olfactory display. In *SIGGRAPH Asia 2018 Virtual & Augmented Reality*. 1–2.

[8] Alexandra Covaci, Ramona Trestian, Estêvão Bissoli Saleme, Ioan-Sorin Comsa, Gebremariam Assres, Celso AS Santos, and Gheorghita Ghinea. 2019. 360° mulsemedia: A way to improve subjective QoE in 360° videos. In *Proceedings of the 27th ACM International Conference on Multimedia*. 2378–2386.

[9] Huong Q Dinh, Neff Walker, Larry F Hodges, Chang Song, and Akira Kobayashi. 1999. Evaluating the importance of multi-sensory input on memory and the sense of presence in virtual environments. In *Proceedings IEEE Virtual Reality (Cat. No. 99CB36316)*. IEEE, 222–228.

[10] Bernadette Emsenhuber and Alois Ferscha. 2009. Olfactory interaction zones. In *Conf. on Pervasive Computing*.

[11] Morteza Gharib, Edmond Rambod, and Karim Shariff. 1998. A universal time scale for vortex ring formation. *Journal of Fluid Mechanics* 360 (1998), 121–140.

[12] Ari Glezer. 1988. The formation of vortex rings. *The Physics of fluids* 31, 12 (1988), 3532–3542.

[13] Sidhant Gupta, Dan Morris, Shwetak N Patel, and Desney Tan. 2013. Airwave: Non-contact haptic feedback using air vortex rings. In *Proceedings of the 2013 ACM international joint conference on Pervasive and ubiquitous computing*. 419–428.

[14] Usman Haque. 2004. Scents of Space: an interactive smell system. In *ACM SIGGRAPH 2004 Sketches*. 35.

[15] Keisuke Hasegawa, Liwei Qiu, and Hiroyuki Shinoda. 2018. Midair ultrasound fragrance rendering. *IEEE transactions on visualization and computer graphics* 24, 4 (2018), 1477–1485.

[16] Kazuki Hashimoto and Takamichi Nakamoto. 2016. Tiny olfactory display using surface acoustic wave device and micropumps for wearable applications. *IEEE Sensors Journal* 16, 12 (2016), 4974–4980.

[17] Morton Leonard Heilig. 1992. El cine del futuro: The cinema of the future. *Presence: Teleoperators & Virtual Environments* 1, 3 (1992), 279–294.

[18] Ami Kadowaki, Junta Sato, Yuichi Bannai, and Ken-ichi Okada. 2007. Presentation technique of scent to avoid olfactory adaptation. In *17th International Conference on Artificial Reality and Telexistence (ICAT 2007)*. IEEE, 97–104.

[19] Takahiro Kusabuka and Shinichiro Eitoku. 2019. Lucciola: Presenting Aerial Images by Generating a Fog Screenat Any Point in the Same 3D Space as a User. In *SIGGRAPH Asia 2019 Posters*. 1–2.

[20] Benjamin J Li and Jeremy N Bailenson. 2018. Exploring the influence of haptic and olfactory cues of a virtual donut on satiation and eating behavior. *Presence* 26, 03 (2018), 337–354.

[21] Haruka Matsukura, Tomohiko Nihei, and Hiroshi Ishida. 2011. Multi-sensorial field display: Presenting spatial distribution of airflow and odor. In *2011 IEEE Virtual Reality Conference*. IEEE, 119–122.

[22] Haruka Matsukura, Akira Ohno, and Hiroshi Ishida. 2010. Fluid dynamic considerations for realistic odor presentation using olfactory display. *Presence: Teleoperators and Virtual Environments* 19, 6 (2010), 513–526.

[23] Haruka Matsukura, Tatsuhiro Yoneda, and Hiroshi Ishida. 2012. Smelling screen: Technique to present a virtual odor source at an arbitrary position on a screen. In *2012 IEEE Virtual Reality Workshops (VRW)*. IEEE, 127–128.

[24] Koji Murai, Takafumi Serizawa, and Yasuyuki Yanagida. 2011. Localized scent presentation to a walking person by using scent projectors. In *2011 IEEE International Symposium on VR Innovation*. IEEE, 67–70.

[25] Niall Murray, Brian Lee, Yuansong Qiao, and Gabriel-Miro Muntean. 2016. Olfaction-enhanced multimedia: A survey of application domains, displays, and research challenges. *ACM Computing Surveys (CSUR)* 48, 4 (2016), 1–34.

[26] Fumitaka Nakaizumi, Haruo Noma, Kenichi Hosaka, and Yasuyuki Yanagida. 2006. SpotScents: A novel method of natural scent delivery using multiple scent projectors. In *IEEE Virtual Reality Conference (VR 2006)*. IEEE, 207–214.

[27] Takamichi Nakamoto, Tatsuya Hirasawa, and Yukiko Hanyu. 2020. Virtual environment with smell using wearable olfactory display and computational fluid dynamics simulation. In *2020 IEEE Conference on Virtual Reality and 3D User Interfaces (VR)*. IEEE, 713–720.

[28] Takuji Narumi, Takashi Kajinami, Shinya Nishizaka, Tomohiro Tanikawa, and Michitaka Hirose. 2011. Pseudo-gustatory display system based on cross-modal integration of vision, olfaction and gustation. In *2011 IEEE Virtual Reality Conference*. IEEE, 127–130.

[29] Daisuke Noguchi, Sayumi Sugimoto, Yuichi Bannai, and Ken-ichi Okada. 2011. Time characteristics of olfaction in a single breath. In *Proceedings of the SIGCHI Conference on Human Factors in Computing Systems*. 83–92.

[30] ChangHoon Park, Heedong Ko, Ig-Jae Kim, Sang Chul Ahn, Yong-Moo Kwon, and Hyoung-Gon Kim. 2002. The making of Kyongju VR theatre. In *Proceedings IEEE Virtual Reality 2002*. IEEE, 269–270.

[31] Spencer B Perry and Kent L Gee. 2014. The acoustically driven vortex cannon. *The Physics Teacher* 52, 3 (2014), 146–147.

[32] Nimesha Ranasinghe, Pravar Jain, Nguyen Thi Ngoc Tram, Koon Chuan Raymond Koh, David Tolley, Shienny Karwita, Lin Lien-Ya, Yan Liangkun, Kala Shamaiah, Chow Eason Wai Tung, et al. 2018. Season traveller: Multisensory narration for enhancing the virtual reality experience. In *Proceedings of the 2018 CHI Conference on Human Factors in Computing Systems*. 1–13.

[33] R Andrew Russell. 2011. Air vortex ring communication between mobile robots. *Robotics and Autonomous Systems* 59, 2 (2011), 65–73.

[34] Sue Ann Seah, Diego Martinez Plasencia, Peter D Bennett, Abhijit Karnik, Vlad Stefan Otrocol, Jarrod Knibbe, Andy Cockburn, and Sriram Subramanian. 2014. SensaBubble: a chrono-sensory mid-air display of sight and smell. In *Proceedings of the SIGCHI Conference on Human Factors in Computing Systems*. 2863–2872.

[35] Karim Shariff and Anthony Leonard. 1992. Vortex rings. *Annual Review of Fluid Mechanics* 24, 1 (1992), 235–279.

[36] Rajinder Sodhi, Ivan Poupyrev, Matthew Glisson, and Ali Israr. 2013. AIREAL: interactive tactile experiences in free air. *ACM Transactions on Graphics (TOG)* 32, 4 (2013), 1–10.

[37] Sayumi Sugimoto, Daisuke Noguchi, Yuichi Bannnai, and Kenichi Okada. 2010. Ink jet olfactory display enabling instantaneous switches of scents. In *Proceedings of the 18th ACM international conference on Multimedia*. 301–310.

[38] Kentaro Tominaga, Shinkuro Honda, Takaharu Ohsawa, Hiroshi Shigeno, Ken-ichi Okada, and Yutaka Matsushita. 2001. " Friend Park"-expression of the wind and the scent on virtual space. In *Proceedings Seventh International Conference on Virtual Systems and Multimedia*. IEEE, 507–515.

[39] Yanan Wang, Judith Amores, and Pattie Maes. 2020. On-face olfactory interfaces. In *Proceedings of the 2020 CHI Conference on Human Factors in Computing Systems*. 1–9.

[40] Carl J Watkins. 2002. Methods and apparatus for localized delivery of scented aerosols. US Patent 6,357,726.

[41] Tomoya Yamada, Satoshi Yokoyama, Tomohiro Tanikawa, Koichi Hirota, and Michitaka Hirose. 2006. Wearable olfactory display: Using odor in outdoor environment. In *IEEE Virtual Reality Conference (VR 2006)*. IEEE, 199–206.

[42] Yasuyuki Yanagida. 2012. A survey of olfactory displays: Making and delivering scents. In *SENSORS, 2012 IEEE*. IEEE, 1–4.

[43] Yasuyuki Yanagida, Takuya Adachi, Tsutomu Miyasato, Akira Tomono, Shinjiro Kawato, Haruo Noma, and Kenichi Hosaka. 2005. Integrating a projection-based olfactory display with interactive audio-visual contents. In *HCI International*.

[44] Yasuyuki Yanagida, Masashi Kajima, Shunpei Suzuki, and Yuya Yoshioka. 2013. Pilot study for generating dynamic olfactory field using scent projectors. In *2013 IEEE Virtual Reality (VR)*. IEEE, 151–152.

[45] Yasuyuki Yanagida, Shinjiro Kawato, Haruo Noma, Akira Tomono, and N Tesutani. 2004. Projection based olfactory display with nose tracking. In *IEEE Virtual Reality 2004*. IEEE, 43–50.

[46] Yasuyuki Yanagida, Tatsuya Tanakamaru, Hiroki Nagayanagi, Yuki Nomura, and Toshimasa Aritake. 2012. Flat-shaped, front-face-drive scent projector. In *2012 IEEE Virtual Reality Workshops (VRW)*. IEEE, 159–160.